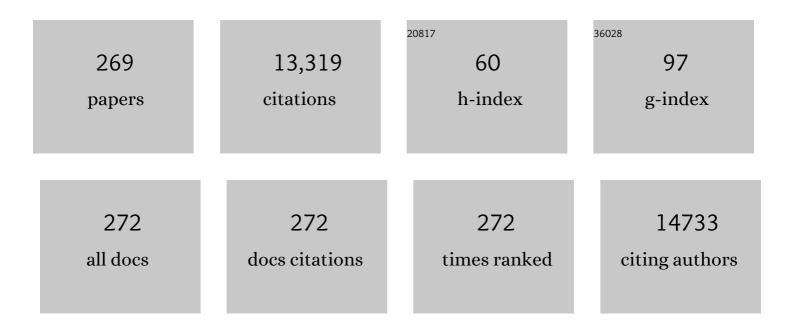
List of Publications by Year in descending order

Source: https://exaly.com/author-pdf/6755389/publications.pdf Version: 2024-02-01



ARDOLDEZA SIMCHI

#	Article	IF	CITATIONS
1	A comprehensive review on planar boron nitride nanomaterials: From 2D nanosheets towards 0D quantum dots. Progress in Materials Science, 2022, 124, 100884.	32.8	59
2	Concurrent electrophoretic deposition of enzyme-laden chitosan/graphene oxide composite films for biosensing. Materials Letters, 2022, 308, 131228.	2.6	8
3	Efficient Electrocatalytic Overall Water Splitting on a Copper-Rich Alloy: An Electrochemical Study. Energy & Fuels, 2022, 36, 4502-4509.	5.1	11
4	Effect of silica encapsulation on the stability and photoluminescence emission of FAPbI3 nanocrystals for white-light-emitting perovskite diodes. Journal of Alloys and Compounds, 2022, 907, 164465.	5.5	4
5	Ultrafast Graphitization and Reduction of Spongy Graphene Oxide by Low-Energy Electromagnetic Radiation to Boost the Performance and Stability of Carbon-Based Supercapacitors. ACS Applied Energy Materials, 2022, 5, 367-379.	5.1	5
6	Multilayered Mesoporous Composite Nanostructures for Highly Sensitive Label-Free Quantification of Cardiac Troponin-I. Biosensors, 2022, 12, 337.	4.7	11
7	Graphene-based polymer nanocomposites in biomedical applications. , 2022, , 199-245.		2
8	Magneto-fluorescent contrast agents based on carbon Dots@Ferrite nanoparticles for tumor imaging. Journal of Magnetism and Magnetic Materials, 2022, 561, 169686.	2.3	7
9	Seedless growth of two-dimensional disc-shaped WS2 layers by chemical vapor deposition. Materials Chemistry and Physics, 2021, 257, 123837.	4.0	4
10	Nanoengineered shear-thinning and bioprintable hydrogel as a versatile platform for biomedical applications. Biomaterials, 2021, 267, 120476.	11.4	76
11	New insight into reaction mechanisms of TiCl4 for the synthesis of TiO2 nanoparticles in H2O-assisted atmospheric-pressure CVS process. Materials Science and Engineering B: Solid-State Materials for Advanced Technology, 2021, 264, 114958.	3.5	7
12	Efficient FAPbI ₃ –PbS quantum dot graphene-based phototransistors. New Journal of Chemistry, 2021, 45, 15285-15293.	2.8	6
13	Biomimetic nanoengineered scaffold for enhanced full-thickness cutaneous wound healing. Acta Biomaterialia, 2021, 124, 191-204.	8.3	72
14	Green Electrospun Membranes Based on Chitosan/Amino-Functionalized Nanoclay Composite Fibers for Cationic Dye Removal: Synthesis and Kinetic Studies. ACS Omega, 2021, 6, 10816-10827.	3.5	24
15	Electrocatalytic hydrogen evolution reaction on graphene supported transition metal-organic frameworks. Inorganic Chemistry Communication, 2021, 127, 108525.	3.9	38
16	Stable Photodetectors Based on Formamidinium Lead Iodide Quantum Well Perovskite Nanoparticles Fabricated with Excess Organic Cations. ACS Applied Nano Materials, 2021, 4, 7788-7799.	5.0	9
17	3D self-supporting mixed transition metal oxysulfide nanowires on porous graphene networks for oxygen evolution reaction in alkaline solution. Journal of Electroanalytical Chemistry, 2021, 893, 115308.	3.8	10
18	Efficient electrocatalytic oxidation of water and glucose on dendritic-shaped multicomponent transition metals/spongy graphene composites. Electrochimica Acta, 2021, 386, 138484.	5.2	16

#	Article	IF	CITATIONS
19	Facile synthesis and self-assembling of transition metal phosphide nanosheets to microspheres as a high-performance electrocatalyst for full water splitting. Journal of Alloys and Compounds, 2021, 875, 160049.	5.5	26
20	High Yield of CO and Synchronous S Recovery from the Conversion of CO ₂ and H ₂ S in Natural Gas Based on a Novel Electrochemical Reactor. Environmental Science & Technology, 2021, 55, 14854-14862.	10.0	14
21	Self-assembly, stability, and photoresponse of PbS quantum dot films capped with mixed halide perovskite ligands. Materials Research Bulletin, 2021, 147, 111648.	5.2	3
22	Processing and Properties of Nanofibrous Bacterial Cellulose-Containing Polymer Composites: A Review of Recent Advances for Biomedical Applications. Polymer Reviews, 2020, 60, 144-170.	10.9	101
23	Surface/edge functionalized boron nitride quantum dots: Spectroscopic fingerprint of bandgap modification by chemical functionalization. Ceramics International, 2020, 46, 978-985.	4.8	31
24	Nanoporous composites of activated carbon-metal organic frameworks for organic dye adsorption: Synthesis, adsorption mechanism and kinetics studies. Journal of Industrial and Engineering Chemistry, 2020, 81, 405-414.	5.8	169
25	Biomimetic proteoglycan nanoparticles for growth factor immobilization and delivery. Biomaterials Science, 2020, 8, 1127-1136.	5.4	18
26	Submerged friction stir welding of dissimilar joints between an Al-Mg alloy and low carbon steel: Thermo-mechanical modeling, microstructural features, and mechanical properties. Journal of Manufacturing Processes, 2020, 50, 68-79.	5.9	61
27	Extraction of Hydroxyapatite Nanostructures from Marine Wastes for the Fabrication of Biopolymer-Based Porous Scaffolds. Marine Drugs, 2020, 18, 26.	4.6	19
28	Clucose cross-linked hydrogels conjugate HA nanorods as bone scaffolds: Green synthesis, characterization and in vitro studies. Materials Chemistry and Physics, 2020, 242, 122515.	4.0	22
29	Core-sheath gelatin based electrospun nanofibers for dual delivery release of biomolecules and therapeutics. Materials Science and Engineering C, 2020, 108, 110432.	7.3	43
30	A new procedure for the fabrication of dissimilar joints through injection of colloidal nanoparticles during friction stir processing: Proof concept for AA6062/PMMA joints. Journal of Manufacturing Processes, 2020, 49, 335-343.	5.9	40
31	Modeling and experimental validation of material flow during FSW of polycarbonate. Materials Today Communications, 2020, 22, 100796.	1.9	42
32	Processing and characterizations of polycarbonate/alumina nanocomposites by additive powder fed friction stir processing. Thin-Walled Structures, 2020, 157, 107086.	5.3	26
33	Robust water splitting on staggered gap heterojunctions based on WO3â^–WS2–MoS2 nanostructures. Renewable Energy, 2020, 162, 504-512.	8.9	13
34	Sensitive Voltammetric Detection of Melatonin in Pharmaceutical Products by Highly Conductive Porous Graphene-Gold Composites. ACS Sustainable Chemistry and Engineering, 2020, 8, 18224-18236.	6.7	11
35	Self-Powered Wearable Piezoelectric Sensors Based on Polymer Nanofiber–Metal–Organic Framework Nanoparticle Composites for Arterial Pulse Monitoring. ACS Applied Nano Materials, 2020, 3, 8742-8752.	5.0	88
36	Friction Stir Welding and Friction Spot Stir Welding Processes of Polymers—State of the Art. Materials, 2020, 13, 2291.	2.9	54

#	Article	IF	CITATIONS
37	Composites of Reduced Graphene Oxide/Nickel Submicrorods for Non-Enzymatic Electrochemical Biosensing: Application to Amperometric Glucose Detection. Journal of the Electrochemical Society, 2020, 167, 087513.	2.9	3
38	Evaluation of a polymer-steel laminated sheet composite structure produced by friction stir additive manufacturing (FSAM) technology. Polymer Testing, 2020, 90, 106690.	4.8	50
39	Solution Processing and Self-Organization of PbS Quantum Dots Passivated with Formamidinium Lead Iodide (FAPbI ₃). ACS Omega, 2020, 5, 15746-15754.	3.5	12
40	<i>In situ</i> synthesis of quasi-needle-like bimetallic organic frameworks on highly porous graphene scaffolds for efficient electrocatalytic water oxidation. Chemical Communications, 2020, 56, 3135-3138.	4.1	47
41	First demonstration of photoelectrochemical water splitting by commercial W–Cu powder metallurgy parts converted to highly porous 3D WO3/W skeletons. International Journal of Hydrogen Energy, 2020, 45, 6369-6379.	7.1	8
42	Review—Textile Based Chemical and Physical Sensors for Healthcare Monitoring. Journal of the Electrochemical Society, 2020, 167, 037546.	2.9	115
43	Effect of Photoelectrochemical Activity of ZnO-Graphene Thin Film on the Corrosion of Carbon Steel and 304 Stainless Steel. Journal of Materials Engineering and Performance, 2020, 29, 497-505.	2.5	16
44	Review—Towards the Two-Dimensional Hexagonal Boron Nitride (2D h-BN) Electrochemical Sensing Platforms. Journal of the Electrochemical Society, 2020, 167, 126513.	2.9	41
45	Electrocatalytic Oxidation of Ethanol on Flexible Threeâ€dimensional Interconnected Nickel/Gold Composite Foams in Alkaline Media. Electroanalysis, 2019, 31, 504-511.	2.9	11
46	Friction stir welding of polycarbonate lap joints: Relationship between processing parameters and mechanical properties. Polymer Testing, 2019, 79, 105999.	4.8	50
47	New approaches in lowering the gas-phase synthesis temperature of TiO2 nanoparticles by H2O-assisted atmospheric pressure CVS process. Journal of Materials Research and Technology, 2019, 8, 3024-3035.	5.8	6
48	Synthesis, First-Principle Simulation, and Application of Three-Dimensional Ceria Nanoparticles/Graphene Nanocomposite for Non-Enzymatic Hydrogen Peroxide Detection. Journal of the Electrochemical Society, 2019, 166, H3167-H3174.	2.9	30
49	Effect of copper on the thermal stability and non-isothermal crystallization behavior of Al86Ni10-xCuxRE4 (x = 0.5–2.5) amorphous alloys prepared by melt spinning. Journal of Non-Crystalline Solids, 2019, 506, 46-50.	3.1	11
50	Kinetics and adsorptive study of organic dye removal using water-stable nanoscale metal organic frameworks. Materials Chemistry and Physics, 2019, 233, 267-275.	4.0	54
51	Modification of bacterial cellulose/keratin nanofibrous mats by a tragacanth gum-conjugated hydrogel for wound healing. International Journal of Biological Macromolecules, 2019, 134, 280-289.	7.5	52
52	Yttrium Hexacyanoferrate Microflowers on Freestanding Three-Dimensional Graphene Substrates for Ascorbic Acid Detection. ACS Applied Nano Materials, 2019, 2, 2212-2221.	5.0	32
53	Ligand functionalized copper nanoclusters for versatile applications in catalysis, sensing, bioimaging, and optoelectronics. Materials Chemistry Frontiers, 2019, 3, 2326-2356.	5.9	75
54	Dispute in photocatalytic and photoluminescence behavior in ZnO/graphene oxide core-shell nanoparticles. Materials Letters, 2019, 240, 117-120.	2.6	6

#	Article	IF	CITATIONS
55	Fast and ultra-sensitive voltammetric detection of lead ions by two-dimensional graphitic carbon nitride (g-C3N4) nanolayers as glassy carbon electrode modifier. Measurement: Journal of the International Measurement Confederation, 2019, 134, 679-687.	5.0	62
56	Fabrication and Characterization of Core-Shell Electrospun Fibrous Mats Containing Medicinal Herbs for Wound Healing and Skin Tissue Engineering. Marine Drugs, 2019, 17, 27.	4.6	62
57	An investigation on the dissimilar friction stir welding of T-joints between AA5754 aluminum alloy and poly(methyl methacrylate). Thin-Walled Structures, 2019, 135, 376-384.	5.3	57
58	Effect of graphene oxide nanosheets on visible light-assisted antibacterial activity of vertically-aligned copper oxide nanowire arrays. Journal of Colloid and Interface Science, 2018, 521, 119-131.	9.4	45
59	Graphene-mediated self-assembly of gold nanorods into long fibers with controllable optical properties. Materials Letters, 2018, 224, 13-17.	2.6	5
60	Enzymatic biosensing by covalent conjugation of enzymes to 3D-networks of graphene nanosheets on arrays of vertically aligned gold nanorods: Application to voltammetric glucose sensing. Mikrochimica Acta, 2018, 185, 178.	5.0	12
61	Effects of alumina nanoparticles on the microstructure, strength and wear resistance of poly(methyl) Tj ETQq1 I Behavior of Biomedical Materials, 2018, 79, 246-253.	0.78431 3.1	4 rgBT /Over 62
62	Friction-stir lap-joining of aluminium-magnesium/poly-methyl-methacrylate hybrid structures: thermo-mechanical modelling and experimental feasibility study. Science and Technology of Welding and Joining, 2018, 23, 35-49.	3.1	73
63	Toughening mechanisms of SiC-bonded CNT bulk nanocomposites prepared by spark plasma sintering. International Journal of Refractory Metals and Hard Materials, 2018, 71, 61-69.	3.8	8
64	Experimental and thermomechanical analysis of friction stir welding of poly(methyl methacrylate) sheets. Science and Technology of Welding and Joining, 2018, 23, 209-218.	3.1	60
65	Curcumin loading potentiates the neuroprotective efficacy of Fe3O4 magnetic nanoparticles in cerebellum cells of schizophrenic rats. Biomedicine and Pharmacotherapy, 2018, 108, 1244-1252.	5.6	25
66	Dual-Sensitive Hydrogel Nanoparticles Based on Conjugated Thermoresponsive Copolymers and Protein Filaments for Triggerable Drug Delivery. ACS Applied Materials & Interfaces, 2018, 10, 19336-19346.	8.0	42
67	Developing seedless growth of atomically thin semiconductor layers: Application to transition metal dichalcogenides. Ceramics International, 2018, 44, 15795-15803.	4.8	6
68	Experimental and thermomechanical analysis of the effect of tool pin profile on the friction stir welding of poly(methyl methacrylate) sheets. Journal of Manufacturing Processes, 2018, 34, 412-423.	5.9	74
69	Mechanochemical Green Synthesis of Exfoliated Edge-Functionalized Boron Nitride Quantum Dots: Application to Vitamin C Sensing through Hybridization with Gold Electrodes. ACS Applied Materials & Interfaces, 2018, 10, 28819-28827.	8.0	55
70	Injectable polyethylene glycol-laponite composite hydrogels as articular cartilage scaffolds with superior mechanical and rheological properties. International Journal of Polymeric Materials and Polymeric Biomaterials, 2017, 66, 105-114.	3.4	40
71	High-quality organohalide lead perovskite films fabricated by layer-by-layer alternating vacuum deposition for high efficiency photovoltaics. Materials Chemistry Frontiers, 2017, 1, 1520-1525.	5.9	33
72	In-situ solvothermal processing of polycaprolactone/hydroxyapatite nanocomposites with enhanced mechanical and biological performance for bone tissue engineering. Bioactive Materials, 2017, 2, 146-155.	15.6	36

#	Article	IF	CITATIONS
73	Reactive friction-stir processing of nanocomposites: Effects of thermal history on microstructure–mechanical property relationships. Materials Science and Technology, 2017, 33, 1776-1789.	1.6	13
74	Organic Halides and Nanocone Plastic Structures Enhance the Energy Conversion Efficiency and Self-Cleaning Ability of Colloidal Quantum Dot Photovoltaic Devices. Journal of Physical Chemistry C, 2017, 121, 9757-9765.	3.1	22
75	The role of microstructural features on the electrical resistivity and mechanical properties of powder metallurgy Al-SiC-Al 2 O 3 nanocomposites. Materials and Design, 2017, 130, 26-36.	7.0	61
76	Three-dimensional hybrid graphene/nickel electrodes on zinc oxide nanorod arrays as non-enzymatic glucose biosensors. Sensors and Actuators B: Chemical, 2017, 251, 462-471.	7.8	65
77	Temporary skin grafts based on hybrid graphene oxide-natural biopolymer nanofibers as effective wound healing substitutes: pre-clinical and pathological studies in animal models. Journal of Materials Science: Materials in Medicine, 2017, 28, 73.	3.6	62
78	Biochemical mechanisms of dose-dependent cytotoxicity and ROS-mediated apoptosis induced by lead sulfide/graphene oxide quantum dots for potential bioimaging applications. Scientific Reports, 2017, 7, 12896.	3.3	47
79	Self-limited growth of large-area monolayer graphene films by low pressure chemical vapor deposition for graphene-based field effect transistors. Ceramics International, 2017, 43, 15010-15017.	4.8	11
80	Effects of functionalization and side defects on single-photon emission in boron nitride quantum dots. Physical Review B, 2017, 96, .	3.2	23
81	Surface modifications of an aluminum-magnesium alloy through reactive stir friction processing with titanium oxide nanoparticles for enhanced sliding wear resistance. Surface and Coatings Technology, 2017, 309, 114-123.	4.8	59
82	On the biological performance of graphene oxide-modified chitosan/polyvinyl pyrrolidone nanocomposite membranes: In vitro and in vivo effects of graphene oxide. Materials Science and Engineering C, 2017, 70, 121-131.	7.3	83
83	Influence of hard inclusions on microstructural characteristics and textural components during dissimilar friction-stir welding of an PM Al–Al ₂ O ₃ –SiC hybrid nanocomposite with AA1050 alloy. Science and Technology of Welding and Joining, 2017, 22, 412-427.	3.1	38
84	Nanostructured coatings for biomaterials. , 2017, , 191-210.		1
85	Electrospinning of Nanodiamond-Modified Polysaccharide Nanofibers with Physico-Mechanical Properties Close to Natural Skins. Marine Drugs, 2016, 14, 128.	4.6	56
86	Hybrid cross-linked hydrogels based on fibrous protein/block copolymers and layered silicate nanoparticles: tunable thermosensitivity, biodegradability and mechanical durability. RSC Advances, 2016, 6, 62944-62957.	3.6	67
87	Effect of graphene oxide nanosheets on the physico-mechanical properties of chitosan/bacterial cellulose nanofibrous composites. Composites Part A: Applied Science and Manufacturing, 2016, 85, 113-122.	7.6	67
88	High Antimicrobial Activity and Low Human Cell Cytotoxicity of Core–Shell Magnetic Nanoparticles Functionalized with an Antimicrobial Peptide. ACS Applied Materials & Interfaces, 2016, 8, 11366-11378.	8.0	56
89	Surface passivation of lead sulfide nanocrystals with low electron affinity metals: photoluminescence and photovoltaic performance. Physical Chemistry Chemical Physics, 2016, 18, 12086-12092.	2.8	18
90	Similar and dissimilar friction-stir welding of an PM aluminum-matrix hybrid nanocomposite and commercial pure aluminum: Microstructure and mechanical properties. Materials Science & Engineering A: Structural Materials: Properties, Microstructure and Processing, 2016, 666, 225-237.	5.6	62

#	Article	IF	CITATIONS
91	Effect of alumina nanoparticles on the microstructure and mechanical durability of meltspun lead-free solders based on tin alloys. Journal of Alloys and Compounds, 2016, 688, 143-155.	5.5	42
92	Effect of silicon carbide nanoparticles on hot deformation of ultrafine-grained aluminium nanocomposites prepared by hot powder extrusion process. Powder Metallurgy, 2016, 59, 262-270.	1.7	4
93	Smart Polymeric Hydrogels for Cartilage Tissue Engineering: A Review on the Chemistry and Biological Functions. Biomacromolecules, 2016, 17, 3441-3463.	5.4	201
94	Physicochemical and antibacterial properties of chitosanâ€polyvinylpyrrolidone films containing selfâ€organized graphene oxide nanolayers. Journal of Applied Polymer Science, 2016, 133, .	2.6	49
95	A general two-step chemical vapor deposition procedure to synthesize highly crystalline transition metal dichalcogenides: A case study of MoS2. Materials Research Bulletin, 2016, 76, 473-478.	5.2	8
96	Electrophoretic deposition and sintering of a nanostructured manganese–cobalt spinel coating for solid oxide fuel cell interconnects. Ceramics International, 2016, 42, 6648-6656.	4.8	31
97	Spark plasma sintering of a multilayer thermal barrier coating on Inconel 738 superalloy: Microstructural development and hot corrosion behavior. Ceramics International, 2016, 42, 2770-2779.	4.8	37
98	Surface Modifications of Titanium Implants by Multilayer Bioactive Coatings with Drug Delivery Potential: Antimicrobial, Biological, and Drug Release Studies. Jom, 2016, 68, 1100-1108.	1.9	23
99	Fatigue fracture of friction-stir processed Al–Al3Ti–MgO hybrid nanocomposites. International Journal of Fatigue, 2016, 87, 266-278.	5.7	45
100	Chemical processing of three-dimensional graphene networks on transparent conducting electrodes for depleted-heterojunction quantum dot solar cells. Chemical Communications, 2016, 52, 323-326.	4.1	40
101	Nanomedicine applications in orthopedic medicine: state of the art. International Journal of Nanomedicine, 2015, 10, 6039.	6.7	35
102	Development of Chitosan/Bacterial Cellulose Composite Films Containing Nanodiamonds as a Potential Flexible Platform for Wound Dressing. Materials, 2015, 8, 6401-6418.	2.9	83
103	Antibiotic-loaded chitosan–Laponite films for local drug delivery by titanium implants: cell proliferation and drug release studies. Journal of Materials Science: Materials in Medicine, 2015, 26, 269.	3.6	53
104	Reactive friction stir processing of AA 5052–TiO ₂ nanocomposite: process–microstructure–mechanical characteristics. Materials Science and Technology, 2015, 31, 426-435.	1.6	69
105	Physicochemical properties of hybrid graphene–lead sulfide quantum dots prepared by supercritical ethanol. Journal of Nanoparticle Research, 2015, 17, 1.	1.9	35
106	Hot deformation behavior of an aluminum-matrix hybrid nanocomposite fabricated by friction stir processing. Materials Science & Engineering A: Structural Materials: Properties, Microstructure and Processing, 2015, 626, 458-466.	5.6	48
107	Quasi Core/Shell Lead Sulfide/Graphene Quantum Dots for Bulk Heterojunction Solar Cells. Journal of Physical Chemistry C, 2015, 119, 18886-18895.	3.1	50
108	Effects of nanometric inclusions on the microstructural characteristics and strengthening of a friction-stir processed aluminum–magnesium alloy. Materials Science & Engineering A: Structural Materials: Properties, Microstructure and Processing, 2015, 642, 215-229.	5.6	52

#	Article	IF	CITATIONS
109	Supercritical Synthesis and Characterization of Graphene–PbS Quantum Dots Composite with Enhanced Photovoltaic Properties. Industrial & Engineering Chemistry Research, 2015, 54, 7382-7392.	3.7	38
110	Effects of stored strain energy on restoration mechanisms and texture components in an aluminum–magnesium alloy prepared by friction stir processing. Materials Science & Engineering A: Structural Materials: Properties, Microstructure and Processing, 2015, 642, 204-214.	5.6	66
111	Effect of starting materials on the wear performance of NiTi-based composites. Wear, 2015, 334-335, 35-43.	3.1	33
112	Supercritical synthesis and in situ deposition of PbS nanocrystals with oleic acid passivation for quantum dot solar cells. Materials Chemistry and Physics, 2015, 156, 163-169.	4.0	32
113	Nanostructured aluminium titanate (Al2TiO5) particles and nanofibers: Synthesis and mechanism of microstructural evolution. Materials Characterization, 2015, 103, 125-132.	4.4	20
114	A Processing Map for Hot Deformation of an Ultrafine-Grained Aluminum-Magnesium-Silicon Alloy Prepared by Mechanical Milling and Hot Extrusion. Metallurgical and Materials Transactions A: Physical Metallurgy and Materials Science, 2015, 46, 5900-5908.	2.2	2
115	Hybrid zinc oxide/graphene electrodes for depleted heterojunction colloidal quantum-dot solar cells. Physical Chemistry Chemical Physics, 2015, 17, 24412-24419.	2.8	45
116	Fabrication of a highly ordered hierarchically designed porous nanocomposite via indirect 3D printing: Mechanical properties and in vitro cell responses. Materials and Design, 2015, 88, 924-931.	7.0	28
117	Friction stir processing of an aluminum-magnesium alloy with pre-placing elemental titanium powder: In-situ formation of an Al3Ti-reinforced nanocomposite and materials characterization. Materials Characterization, 2015, 108, 102-114.	4.4	75
118	Physicochemical and biological properties of electrodeposited graphene oxide/chitosan films with drug-eluting capacity. Carbon, 2015, 84, 91-102.	10.3	85
119	Cryogenic friction-stir processing of ultrafine-grained Al–Mg–TiO2 nanocomposites. Materials Science & Engineering A: Structural Materials: Properties, Microstructure and Processing, 2015, 620, 471-482.	5.6	89
120	Development of composite silver/nickel nanopastes for low temperature joining of yttria-stabilized zirconia to stainless steels. Ceramics International, 2015, 41, 1815-1822.	4.8	8
121	Effects of Ti-based catalysts on hydrogen desorption kinetics of nanostructured magnesium hydride. International Journal of Hydrogen Energy, 2014, 39, 21007-21014.	7.1	48
122	Microstructure and texture development during friction stir processing of Al–Mg alloy sheets with TiO2 nanoparticles. Materials Science & Engineering A: Structural Materials: Properties, Microstructure and Processing, 2014, 605, 108-118.	5.6	83
123	Flexible bactericidal graphene oxide–chitosan layers for stem cell proliferation. Applied Surface Science, 2014, 301, 456-462.	6.1	126
124	Photo-degradation of organic dye by zinc oxide nanosystems with special defect structure: Effect of the morphology and annealing temperature. Applied Catalysis A: General, 2014, 472, 198-204.	4.3	33
125	Development of fcc-Al nanoparticles during crystallization of amorphous Al–Ni alloys containing mischmetal: Microstructure and hardness evaluation. Materials Science & Engineering A: Structural Materials: Properties, Microstructure and Processing, 2014, 604, 92-97.	5.6	20
126	Non-isothermal kinetic studies of crystallization in amorphous Al86Ni10MM4 alloy. Journal of Non-Crystalline Solids, 2014, 387, 36-40.	3.1	7

#	Article	IF	CITATIONS
127	Strain Rate Sensitivity, Work Hardening, and Fracture Behavior of an Al-Mg TiO2 Nanocomposite Prepared by Friction Stir Processing. Metallurgical and Materials Transactions A: Physical Metallurgy and Materials Science, 2014, 45, 4073-4088.	2.2	45
128	Characterization and antibacterial performance of electrodeposited chitosan–vancomycin composite coatings for prevention of implant-associated infections. Materials Science and Engineering C, 2014, 41, 240-248.	7.3	88
129	Study the Effect of Architectural Modification on Fracture Behavior of Al-DRA Composite. Mechanics of Advanced Materials and Structures, 2014, 21, 662-668.	2.6	0
130	Long-term antibiotic delivery by chitosan-based composite coatings with bone regenerative potential. Applied Surface Science, 2014, 317, 56-66.	6.1	76
131	Size tuning of Agâ€decorated TiO ₂ nanotube arrays for improved bactericidal capacity of orthopedic implants. Journal of Biomedical Materials Research - Part A, 2014, 102, 2625-2635.	4.0	49
132	Extended Quantum Yield: A Dimensionless Factor Including Characteristics of Light Source, Photocatalyst Surface, and Reaction Kinetics in Photocatalytic Systems. Industrial & Engineering Chemistry Research, 2014, 53, 11973-11978.	3.7	8
133	Microstructural characterization of HIP consolidated NiTi–nano Al2O3 composites. Journal of Alloys and Compounds, 2014, 606, 21-26.	5.5	28
134	Microstructure and compressibility of SiC nanoparticles reinforced Cu nanocomposite powders processed by high energy mechanical milling. Ceramics International, 2014, 40, 951-960.	4.8	50
135	Effects of post-annealing on the microstructure and mechanical properties of friction stir processed Al–Mg–TiO2 nanocomposites. Materials & Design, 2014, 63, 30-41.	5.1	42
136	Effect of Morphology-based Defect Structure of ZnO Nanostructures in Photo-Degradation of Organic Dye. Materials Research Society Symposia Proceedings, 2014, 1672, 8.	0.1	1
137	Electrophoretic deposition of functionally-graded NiO–YSZ composite films. Journal of the European Ceramic Society, 2013, 33, 1815-1823.	5.7	28
138	Tissue growth into threeâ€dimensional composite scaffolds with controlled microâ€features and nanotopographical surfaces. Journal of Biomedical Materials Research - Part A, 2013, 101, 2796-2807.	4.0	44
139	An Investigation on the Fatigue Fracture of P/M Al-SiC Nanocomposites. Metallurgical and Materials Transactions A: Physical Metallurgy and Materials Science, 2013, 44, 2662-2671.	2.2	20
140	Nanodiamonds for surface engineering of orthopedic implants: Enhanced biocompatibility in human osteosarcoma cell culture. Diamond and Related Materials, 2013, 40, 107-114.	3.9	33
141	Effect of nano Al2O3 addition on mechanical properties and wear behavior of NiTi intermetallic. Materials & Design, 2013, 51, 375-382.	5.1	32
142	Fabrication, characterization and mechanical properties of hybrid composites of copper using the nanoparticulates of SiC and carbon nanotubes. Materials Science & Engineering A: Structural Materials: Properties, Microstructure and Processing, 2013, 572, 83-90.	5.6	73
143	MECHANICAL-ACTIVATED PHASE FORMATION OF NiTi IN THE PRESENCE OF NANOPARTICLES. Nano, 2013, 08, 1350048.	1.0	10
144	Friction stir welding of a P/M Al–Al2O3 nanocomposite: Microstructure and mechanical properties. Materials Science & Engineering A: Structural Materials: Properties, Microstructure and Processing, 2013, 585, 222-232.	5.6	85

#	Article	IF	CITATIONS
145	Selfâ€Assembled, Nanowire Network Electrodes for Depleted Bulk Heterojunction Solar Cells. Advanced Materials, 2013, 25, 1769-1773.	21.0	102
146	Effect of nanoparticle content on the microstructural and mechanical properties of nano-SiC dispersed bulk ultrafine-grained Cu matrix composites. Materials & Design, 2013, 52, 881-887.	5.1	91
147	Microstructural development and mechanical properties of nanostructured copper reinforced with SiC nanoparticles. Materials Science & Engineering A: Structural Materials: Properties, Microstructure and Processing, 2013, 568, 33-39.	5.6	57
148	Joint Mapping of Mobility and Trap Density in Colloidal Quantum Dot Solids. ACS Nano, 2013, 7, 5757-5762.	14.6	30
149	Microstructure, strengthening mechanisms and hot deformation behavior of an oxide-dispersion strengthened UFG Al6063 alloy. Materials Characterization, 2013, 75, 108-114.	4.4	35
150	Warm compaction of metallic powders. , 2013, , 86-108.		9
151	Pyrolytic carbon coating for cytocompatibility of titanium oxide nanoparticles: a promising candidate for medical applications. Nanotechnology, 2012, 23, 045102.	2.6	15
152	Size-controlled synthesis of superparamagnetic iron oxide nanoparticles and their surface coating by gold for biomedical applications. Journal of Magnetism and Magnetic Materials, 2012, 324, 3997-4005.	2.3	106
153	Microstructure and mechanical properties of WC–10Co cemented carbide containing VC or (Ta, Nb)C and fracture toughness evaluation using different models. International Journal of Refractory Metals and Hard Materials, 2012, 31, 141-146.	3.8	44
154	High-temperature deformation and structural restoration of a nanostructured Al alloy. Scripta Materialia, 2012, 66, 911-914.	5.2	13
155	Dynamic restoration and microstructural evolution during hot deformation of a P/M Al6063 alloy. Materials Science & Engineering A: Structural Materials: Properties, Microstructure and Processing, 2012, 542, 56-63.	5.6	31
156	Effects of crystal orientation on the tensile and shear deformation of nickel–silicon interfaces: A molecular dynamics simulation. Materials Science & Engineering A: Structural Materials: Properties, Microstructure and Processing, 2012, 543, 217-223.	5.6	8
157	Photocatalytic activity of TiO2-capped ZnO nanoparticles. Journal of Materials Science: Materials in Electronics, 2012, 23, 361-369.	2.2	7
158	Adsorption and solar light activity of transition-metal doped TiO2 nanoparticles as semiconductor photocatalyst. Journal of Materials Science: Materials in Electronics, 2012, 23, 659-667.	2.2	37
159	Magnetic Resonance Imaging Tracking of Stem Cells in Vivo Using Iron Oxide Nanoparticles as a Tool for the Advancement of Clinical Regenerative Medicine. Chemical Reviews, 2011, 111, 253-280.	47.7	385
160	Molecular Dynamics Investigation of <i>\hat{l}^2</i> -SiC Behavior Under Three-Axial Tensile Loading. Journal of Computational and Theoretical Nanoscience, 2011, 8, 2187-2192.	0.4	1
161	Structural characteristics and desorption properties of nanostructured MgH ₂ synthesised by high energy mechanical milling. Powder Metallurgy, 2011, 54, 480-483.	1.7	5
162	Electrophoretic deposition of chitosan/45S5 Bioglass® composite coatings for orthopaedic applications. Surface and Coatings Technology, 2011, 205, 5260-5268.	4.8	154

#	Article	IF	CITATIONS
163	Effect of particle size on the in vitro bioactivity, hydrophilicity and mechanical properties of bioactive glass-reinforced polycaprolactone composites. Materials Science and Engineering C, 2011, 31, 1526-1533.	7.3	88
164	Phase formation during sintering of nanocrystalline zirconia/stainless steel functionally graded composite layers. Materials Letters, 2011, 65, 523-526.	2.6	10
165	Synthesis of a nanostructured MgH2–Ti alloy composite for hydrogen storage via combined vacuum arc remelting and mechanical alloying. Materials Letters, 2011, 65, 1120-1122.	2.6	19
166	Effect of TiO2 morphology on in vitro bioactivity of polycaprolactone/TiO2 nanocomposites. Materials Letters, 2011, 65, 2530-2533.	2.6	24
167	Uneven shrinkage causes problems for cheaper hardmetal tooling. Metal Powder Report, 2011, 66, 29-32.	0.1	0
168	Densification and microstructural evolution during laser sintering of A356/SiC composite powders. Journal of Materials Science, 2011, 46, 1446-1454.	3.7	16
169	Hot deformation of ultrafine-grained Al6063/Al2O3 nanocomposites. Journal of Materials Science, 2011, 46, 4994-5001.	3.7	22
170	Hydrogen desorption properties of MgH2–TiCr1.2Fe0.6 nanocomposite prepared by high-energy mechanical alloying. Journal of Power Sources, 2011, 196, 4604-4608.	7.8	39
171	Microstructure and Mechanical Properties of Oxide-Dispersion Strengthened Al6063 Alloy with Ultra-Fine Grain Structure. Metallurgical and Materials Transactions A: Physical Metallurgy and Materials Science, 2011, 42, 816-824.	2.2	34
172	A simple model for the size and shape dependent Curie temperature of freestanding Ni and Fe nanoparticles based on the average coordination number and atomic cohesive energy. Chemical Physics, 2011, 383, 1-5.	1.9	18
173	Microstructural features, texture and strengthening mechanisms of nanostructured AA6063 alloy processed by powder metallurgy. Materials Science & Engineering A: Structural Materials: Properties, Microstructure and Processing, 2011, 528, 3981-3989.	5.6	64
174	Recent progress in inorganic and composite coatings with bactericidal capability for orthopaedic applications. Nanomedicine: Nanotechnology, Biology, and Medicine, 2011, 7, 22-39.	3.3	363
175	Effects of particle size, shape and crystal structure on the formation energy of Schottky vacancies in free-standing metal nanoparticles: A model study. Physica B: Condensed Matter, 2011, 406, 3777-3780.	2.7	12
176	Formation mechanism of TiO2 nanoparticles in H2O-assisted atmospheric pressure CVS process. Powder Technology, 2011, 209, 15-24.	4.2	13
177	A plastic-yield compaction model for nanostructured Al6063 alloy and Al6063/Al2O3 nanocomposite powder. Powder Technology, 2011, 211, 215-220.	4.2	20
178	On the Formation of SWCNTs and MWCNTs by Arc-Discharge in Aqueous Solutions: The Role of Iron Charge and Counter Ions. Fullerenes Nanotubes and Carbon Nanostructures, 2011, 19, 317-328.	2.1	1
179	Sintering viscosity and sintering stress of nanostructured WC–Co parts prepared by powder injection moulding. Powder Metallurgy, 2011, 54, 84-88.	1.7	3
180	FORMATION OF CARBON NANOTUBES IN IRON-CATALYZED LIQUID ARCING METHOD: EFFECT OF IRON-ION CHARGE IN THE AQUEOUS MEDIUM. International Journal of Modern Physics B, 2011, 25, 4411-4417.	2.0	1

#	Article	lF	CITATIONS
181	Recent advances in surface engineering of superparamagnetic iron oxide nanoparticles for biomedical applications. Journal of the Iranian Chemical Society, 2010, 7, S1-S27.	2.2	93
182	Interface formation and bond strength in 3Y-TZP/Cr composite bilayers produced by sinter–joining. Materials Science & Engineering A: Structural Materials: Properties, Microstructure and Processing, 2010, 527, 449-453.	5.6	6
183	Creep behavior of hot extruded Al-Al2O3 nanocomposite powder. Materials Science & Engineering A: Structural Materials: Properties, Microstructure and Processing, 2010, 527, 2567-2571.	5.6	23
184	In situ synthesis of nanocrystalline Al6063 matrix nanocomposite powder via reactive mechanical alloying. Materials Science & Engineering A: Structural Materials: Properties, Microstructure and Processing, 2010, 527, 4897-4905.	5.6	23
185	Cosintering of Powder Injection Molding Parts Made from Ultrafine WC-Co and 316L Stainless Steel Powders for Fabrication of Novel Composite Structures. Metallurgical and Materials Transactions A: Physical Metallurgy and Materials Science, 2010, 41, 233-241.	2.2	25
186	Synthesis and cytotoxicity assessment of superparamagnetic iron–gold core–shell nanoparticles coated with polyglycerol. Journal of Colloid and Interface Science, 2010, 345, 64-71.	9.4	57
187	A study of the electrophoretic deposition of Bioglass® suspensions using the Taguchi experimental design approach. Journal of the European Ceramic Society, 2010, 30, 2963-2970.	5.7	59
188	Effect of Fe3+ concentration on MWCNTs formation in liquid arcing method. Physica B: Condensed Matter, 2010, 405, 4344-4349.	2.7	2
189	Templated growth of superparamagnetic iron oxide nanoparticles by temperature programming in the presence of poly(vinyl alcohol). Thin Solid Films, 2010, 518, 4281-4289.	1.8	41
190	Analysis of the compaction behavior of Al–SiC nanocomposites using linear and non-linear compaction equations. Advanced Powder Technology, 2010, 21, 273-278.	4.1	66
191	A new approach for the in vitro identification of the cytotoxicity of superparamagnetic iron oxide nanoparticles. Colloids and Surfaces B: Biointerfaces, 2010, 75, 300-309.	5.0	264
192	Co-sintering of M2/17-4PH Powders for Fabrication of Functional Graded Composite Layers. Journal of Composite Materials, 2010, 44, 417-435.	2.4	16
193	Effect of Alumina Nanoparticles on Hot Strength and Deformation Behaviour of Al-5vol% Al ₂ O ₃ Nanocomposite: Experimental Study and Modelling. Journal of Nanoscience and Nanotechnology, 2010, 10, 2641-2645.	0.9	4
194	Fabrication and characterisation of ultrafine-grained Al-5vol%Al _{2O_{3 nanocomposite. International Journal of Nanomanufacturing, 2010, 5, 341.}}	0.3	2
195	Phase formation and microstructural evolution during sintering of Al–Zn–Mg–Cu alloys. Powder Metallurgy, 2010, 53, 62-70.	1.7	9
196	Effect of nanoscaled reinforcement particles on the structural evolution of aluminium powder during mechanical milling. Powder Metallurgy, 2009, 52, 151-157.	1.7	15
197	Preparation and biological evaluation of [67Ga]-labeled-superparamagnetic nanoparticles in normal rats. Radiochimica Acta, 2009, 97, .	1.2	42
198	Supersolidus liquid phase sintering of Al6061/SiC metal matrix composites. Powder Metallurgy, 2009, 52, 28-35.	1.7	27

#	Article	IF	CITATIONS
199	Effect of rapid solidification on the microstructure and mechanical properties of hot-pressed Al–20Si–5Fe alloys. Materials Characterization, 2009, 60, 1370-1381.	4.4	58
200	Electrophoretic deposition of chitosan. Materials Letters, 2009, 63, 2253-2256.	2.6	128
201	Metal hydrides show potential under stress. Metal Powder Report, 2009, 64, 24-28.	0.1	1
202	Cytotoxicity and Cell Cycle Effects of Bare and Poly(vinyl alcohol) oated Iron Oxide Nanoparticles in Mouse Fibroblasts. Advanced Engineering Materials, 2009, 11, B243.	3.5	54
203	Tensile and fatigue fracture of nanometric alumina reinforced copper with bimodal grain size distribution. Materials Science & Engineering A: Structural Materials: Properties, Microstructure and Processing, 2009, 507, 200-206.	5.6	37
204	Flow stress dependence on the grain size in alumina dispersion-strengthened copper with a bimodal grain size distribution. Materials Science & Engineering A: Structural Materials: Properties, Microstructure and Processing, 2009, 518, 41-46.	5.6	26
205	Study the sintering behavior of nanocrystalline 3Y-TZP/430L stainless-steel composite layers for co-powder injection molding. Journal of Materials Science, 2009, 44, 1264-1274.	3.7	27
206	Microstructural evolution of Al-20Si-5Fe alloy during rapid solidification and hot consolidation. Rare Metals, 2009, 28, 639-645.	7.1	11
207	Master sintering curves of a nanoscale 3Y-TZP powder compacts. Ceramics International, 2009, 35, 547-554.	4.8	82
208	Synergetic effect of Ni and Nb2O5 on dehydrogenation properties of nanostructured MgH2 synthesized by high-energy mechanical alloying. International Journal of Hydrogen Energy, 2009, 34, 7724-7730.	7.1	59
209	Cell toxicity of superparamagnetic iron oxide nanoparticles. Journal of Colloid and Interface Science, 2009, 336, 510-518.	9.4	324
210	Analysis of the effect of reinforcement particles on the compressibility of Al–SiC composite powders using a neural network model. Materials & Design, 2009, 30, 1518-1523.	5.1	52
211	Gas phase synthesis of SnOx nanoparticles and characterization. Journal of Alloys and Compounds, 2009, 470, 289-293.	5.5	9
212	Effect of morphology on the solar photocatalytic behavior of ZnO nanostructures. Journal of Alloys and Compounds, 2009, 485, 616-620.	5.5	49
213	Superparamagnetic Iron Oxide Nanoparticles with Rigid Cross-linked Polyethylene Glycol Fumarate Coating for Application in Imaging and Drug Delivery. Journal of Physical Chemistry C, 2009, 113, 8124-8131.	3.1	164
214	An <i>in vitro</i> study of bare and poly(ethylene glycol)-co-fumarate-coated superparamagnetic iron oxide nanoparticles: a new toxicity identification procedure. Nanotechnology, 2009, 20, 225104.	2.6	110
215	Multiphysics Flow Modeling and in Vitro Toxicity of Iron Oxide Nanoparticles Coated with Poly(vinyl) Tj ETQq1 1	0.784314	Frg <u>g</u> T /Overlo
216	Cytotoxicity of Uncoated and Polyvinyl Alcohol Coated Superparamagnetic Iron Oxide Nanoparticles. Journal of Physical Chemistry C, 2009, 113, 9573-9580.	3.1	128

#	Article	IF	CITATIONS
217	An investigation of the densification and microstructural evolution of M2/316L stepwise graded composite during co-sintering. Journal of Materials Science, 2008, 43, 55-63.	3.7	25
218	Effect of iron particle size on the diffusion bonding of Fe–5%Cu powder compact to wrought carbon steels. Materials & Design, 2008, 29, 411-417.	5.1	23
219	Microinjection moulding of 316L/17-4PH and 316L/Fe powders for fabrication of magnetic–nonmagnetic bimetals. Journal of Materials Processing Technology, 2008, 200, 259-264.	6.3	46
220	Densification and grain growth of nanocrystalline 3Y-TZP during two-step sintering. Journal of the European Ceramic Society, 2008, 28, 2933-2939.	5.7	152
221	Sintering of biocompatible P/M Co–Cr–Mo alloy (F-75) for fabrication of porosity-graded composite structures. Materials Science & Engineering A: Structural Materials: Properties, Microstructure and Processing, 2008, 472, 338-346.	5.6	67
222	Microstructure and mechanical properties of Al–20Si–5Fe–2X (X=Cu, Ni, Cr) alloys produced by melt-spinning. Materials Science & Engineering A: Structural Materials: Properties, Microstructure and Processing, 2008, 492, 443-449.	5.6	41
223	Pressureless Sintering of 3Yâ€TZP/Stainless‣teel Composite Layers. Journal of the American Ceramic Society, 2008, 91, 3493-3503.	3.8	26
224	Abnormal grain growth in alumina dispersion-strengthened copper produced by an internal oxidation process. Scripta Materialia, 2008, 58, 966-969.	5.2	47
225	Effect of SiC particles on the laser sintering of Al–7Si–0.3Mg alloy. Scripta Materialia, 2008, 59, 199-202.	5.2	79
226	Foamability and compressive properties of AlSi7–3Âvol.% SiC–0.5Âwt.% TiH2 powder compact. Materials Letters, 2008, 62, 1561-1564.	2.6	18
227	Effect of C and Cu addition on the densification and microstructure of iron powder in direct laser sintering process. Materials Letters, 2008, 62, 2840-2843.	2.6	23
228	Solid state and liquid phase sintering of mechanically activated W–20wt.% Cu powder mixture. Journal of Alloys and Compounds, 2008, 463, 153-159.	5.5	95
229	Mechanical induced reaction in Al–CuO system for in-situ fabrication of Al based nanocomposites. Journal of Alloys and Compounds, 2008, 465, 151-156.	5.5	28
230	Effect of particle size on the microstructure of rapidly solidified Al–20Si–5Fe–2X (X=Cu, Ni, Cr) powder. Journal of Alloys and Compounds, 2008, 466, 111-118.	5.5	37
231	Optimal Design and Characterization of Superparamagnetic Iron Oxide Nanoparticles Coated with Polyvinyl Alcohol for Targeted Delivery and Imaging. Journal of Physical Chemistry B, 2008, 112, 14470-14481.	2.6	232
232	Investigation on compressibility of Al–SiC composite powders. Powder Metallurgy, 2008, 51, 217-223.	1.7	26
233	Hot deformation of PM Al6061 alloy produced by sintering and powder extrusion. Powder Metallurgy, 2008, 51, 354-360.	1.7	6
234	Effect of reinforcement volume fraction on mechanical alloying of Al–SiC nanocomposite powders. Powder Metallurgy, 2007, 50, 276-282.	1.7	37

#	Article	IF	CITATIONS
235	3D Printing of Biocompatible PM-Materials. Materials Science Forum, 2007, 534-536, 453-456.	0.3	12
236	An Investigation on the Sintering Behavior of High Strength Al-Zn-Mg-Cu Alloy Prepared from Elemental Powders. Materials Science Forum, 2007, 534-536, 489-492.	0.3	4
237	Structural changes during synthesizing of nanostructured W–20wt% Cu composite powder by mechanical alloying. Materials Science & Engineering A: Structural Materials: Properties, Microstructure and Processing, 2007, 445-446, 86-93.	5.6	63
238	Artificial neural network modeling of mechanical alloying process for synthesizing of metal matrix nanocomposite powders. Materials Science & Engineering A: Structural Materials: Properties, Microstructure and Processing, 2007, 466, 274-283.	5.6	40
239	An investigation on the compressibility of aluminum/nano-alumina composite powder prepared by blending and mechanical milling. Materials Science & Engineering A: Structural Materials: Properties, Microstructure and Processing, 2007, 454-455, 89-98.	5.6	137
240	Reactive milling synthesis of nanocrystalline Al–Cu/Al2O3 nanocomposite. Materials Science & Engineering A: Structural Materials: Properties, Microstructure and Processing, 2007, 464, 225-232.	5.6	43
241	Manufacturing of multi-functional micro parts by two-component metal injection moulding. International Journal of Advanced Manufacturing Technology, 2007, 33, 176-186.	3.0	48
242	Determination of the physical and mechanical properties of iron-based powder materials produced by microwave sintering. Powder Metallurgy and Metal Ceramics, 2007, 46, 423-428.	0.8	4
243	Kinetics and mechanisms of nanoparticle formation and growth in vapor phase condensation process. Materials & Design, 2007, 28, 850-856.	5.1	60
244	Behaviour of metal powders during cold and warm compaction. Powder Metallurgy, 2006, 49, 281-287.	1.7	20
245	Effect of ceramic particle addition on the foaming behavior, cell structure and mechanical properties of P/M AlSi7 foam. Materials Science & Engineering A: Structural Materials: Properties, Microstructure and Processing, 2006, 424, 290-299.	5.6	72
246	An investigation on the sintering behavior of 316L and 17-4PH stainless steel powders for graded composites. Materials Science & Engineering A: Structural Materials: Properties, Microstructure and Processing, 2006, 424, 282-289.	5.6	67
247	Structural evolution during mechanical milling of nanometric and micrometric Al2O3 reinforced Al matrix composites. Materials Science & Engineering A: Structural Materials: Properties, Microstructure and Processing, 2006, 428, 159-168.	5.6	192
248	Direct laser sintering of metal powders: Mechanism, kinetics and microstructural features. Materials Science & Engineering A: Structural Materials: Properties, Microstructure and Processing, 2006, 428, 148-158.	5.6	469
249	Densification and microstructural evolution during co-sintering of Ni-base superalloy powders. Metallurgical and Materials Transactions A: Physical Metallurgy and Materials Science, 2006, 37, 2549-2557.	2.2	30
250	DMLS gets an expert once-over. Metal Powder Report, 2006, 61, 10-13.	0.1	2
251	Effect of sintering atmosphere and carbon content on the densification and microstructure of laser-sintered M2 high-speed steel powder. Materials Science & Engineering A: Structural Materials: Properties, Microstructure and Processing, 2005, 403, 290-298.	5.6	55
252	Analysis of the rheological behavior and stability of 316L stainless steel–TiC powder injection molding feedstock. Materials Science & Engineering A: Structural Materials: Properties, Microstructure and Processing, 2005, 407, 105-113.	5.6	66

#	Article	IF	CITATIONS
253	Study of the compaction behavior of composite powders under monotonic and cyclic loading. Composites Science and Technology, 2005, 65, 2094-2104.	7.8	34
254	Investigation of rheological behaviour of 316L stainless steel–3 wt-%TiC powder injection moulding feedstock. Powder Metallurgy, 2005, 48, 144-150.	1.7	20
255	Effects of porosity on delamination wear behaviour of sintered plain iron. Powder Metallurgy, 2004, 47, 73-80.	1.7	64
256	Densification and microstructural evaluation during laser sintering of M2 high speed steel powder. Materials Science and Technology, 2004, 20, 1462-1468.	1.6	65
257	The role of particle size on the laser sintering of iron powder. Metallurgical and Materials Transactions B: Process Metallurgy and Materials Processing Science, 2004, 35, 937-948.	2.1	122
258	Direct laser sintering of iron–graphite powder mixture. Materials Science & Engineering A: Structural Materials: Properties, Microstructure and Processing, 2004, 383, 191-200.	5.6	109
259	Effects of lubrication procedure on the consolidation, sintering and microstructural features of powder compacts. Materials & Design, 2003, 24, 585-594.	5.1	47
260	Effects of laser sintering processing parameters on the microstructure and densification of iron powder. Materials Science & Engineering A: Structural Materials: Properties, Microstructure and Processing, 2003, 359, 119-128.	5.6	311
261	On the development of direct metal laser sintering for rapid tooling. Journal of Materials Processing Technology, 2003, 141, 319-328.	6.3	220
262	Investigation of warm compaction and sintering behaviour of aluminium alloys. Powder Metallurgy, 2003, 46, 159-164.	1.7	19
263	Microstructural changes in Mo steels during sintering and effect on electrical conductivity. Powder Metallurgy, 2002, 45, 307-314.	1.7	4
264	Electrical conductivity and microstructure of sintered ferrous materials: iron–graphite compacts. Powder Metallurgy, 2001, 44, 148-156.	1.7	13
265	Electrical conductivity and microstructure of sintered ferrous materials: sintered iron. Powder Metallurgy, 2000, 43, 209-218.	1.7	10
266	Microstructural modelling of electrical conductivity and mechanical properties of sintered ferrous materials. Powder Metallurgy, 2000, 43, 219-227.	1.7	13
267	Hot Deformation Behavior of P/M Al6061-20% SiC Composite. Materials Science Forum, 0, 534-536, 897-900.	0.3	5
268	Hot Workability of Ultrafine-Grained Aluminum Alloy Produced by Severe Plastic Deformation of Al6063 Powder and Consolidation. Materials Science Forum, 0, 667-669, 979-984.	0.3	1
269	Role of Grain Size and Oxide Dispersion Nanoparticles on the Hot Deformation Behavior of AA6063: Experimental and Artificial Neural Network Modeling Investigations. Metals and Materials International, 0, , 1.	3.4	8